King Saud University

Arabian Journal of Chemistry

www.ksu.edu.sa
www.sciencedirect.com

ORIGINAL ARTICLE

Green synthesis, characterization and photocatalytic application of silver nanoparticles synthesized by various plant extracts

Kishore Chand [a,b], Dianxue Cao [a,*], Diaa Eldin Fouad [a,f], Ahmer Hussain Shah [c], Abdul Qadeer Dayo [d], Kai Zhu [a], Muhammad Nazim Lakhan [a], Ghazanfar Mehdi [e], Shu Dong [a]

[a] Key Laboratory of Superlight Material and Surface Technology, Ministry of Education, Harbin Engineering University, 150001, China
[b] Department of Metallurgy and Materials Engineering, Mehran Unversity of Engineering and Technology, Jamshoro 76020, Pakistan
[c] Department of Textile Engineering, Balochistan University of Information Technology, Engineering and Management Sciences, Quetta 87300, Pakistan
[d] Department of Chemical Engineering, Balochistan University of Information Technology, Engineering and Management Sciences, Quetta 87300, Pakistan
[e] Department of Mechanical Engineering, Hamdard University, Karachi 74600, Pakistan
[f] Ministry of Justice, Forensic Authority, Cairo, Egypt

Abstract Recently, the discharge of effluent containing dyes and other chemicals into river, lakes, and land has become a serious problem which increases the pollution level drastically. The dyes in the effluent are very difficult to be removed by conventional water treatment methods. Thus, there is a great need for more advanced methods that are cost-effective and more efficient. In this study, silver nano particles (AgNps) were synthesized by green method using extracts of onion (O), tomato (T), acacia catechu (C) alone, and mixed COT extracts. The reduction and formation of AgNps and its ions have been characterized by using several techniques, Ultra visible spectroscopy (UV–vis), X-ray diffraction (XRD), transmission electron microscopy (TEM), scanning electron microscopy (SEM)-energy dispersive X-ray spectrometer (EDX), Fourier transmission infrared spectroscopy (FTIR), and dynamic light scattering (DLS). These techniques revealed that the particle sizes of

* Corresponding author.
E-mail address: caodianxue@hrbeu.edu.cn (D. Cao).
Peer review under responsibility of King Saud University.

Production and hosting by Elsevier

synthesized AgNps in all the extracts were ranged in between 5 and 100 nm with a crystalline nature. The synthesized AgNps were used as catalysts for the degradation of three different types of dyes, methyl orange (MO), methyl red (MR), and congo red (CR) in the liquid state. The excellent catalytic application of all the synthesized AgNps on the degradation of the studied dyes was confirmed *via* UV–visible results by studying the reduction in the absorbance maxima value within a very short interval of time. COT synthesized products were found to achieve the best performance for all dyes degradation among all products.

1. Introduction

Nanotechnology is a versatile field that deals with the study and application of materials at the nanoscale. Nanoparticles (Nps) exhibit new and improved properties as compared to bulk counterparts due to change in their characteristics such as shape, size, size distribution and larger surface area to volume ratio (Fouad et al., 2019a, Kalpana et al., 2019). Nowadays, metal Nps have found many applications in the field of science and technology due to their unique electronic, mechanical, optical and magnetic properties (Begum et al., 2009). In recent years, silver nanoparticles (AgNps) have greatly focused the researcher's attention because of their important application as antimicrobial, catalytic, textile fabrics and plastics to eliminate micro-organisms (Fouad et al., 2019b, Kalpana et al., 2019).

In this advanced and populated era, more comfort and ease of life have increased industrial zones and the rate of production is increased day by day because of the peoples' needs. For the need of wearing clothing and fashion changes, different types of textile industries including dying, finishing, leather and weaving use different types of chemicals and dyes for production. The waste water generated in production and processing is disposed off without any treatment which creates many environmental problems for human beings as well as for the aquatic environment. The dyes in the waste water are one of the major group of pollutants. There are many kinds of dyes used in different industries on the large scale, among them the Methyl orange (MO), Methyl red (MR), and Congo Red (CR) are of common class because of their ease of application and basic colors(R.nithya and R.Ragunathan, 2009, Wahi et al., 2005). CR is highly toxic and carcinogenic anionic dye belonging to a group of azo dyes, derived from benzylamine. The Presence of CR dye in the waste water would be very harmful to the aquatic environment. An efficient dye degradation has become a challenging task for environmental engineers as well as scientists. Different methods have been adopted by scientists for degradation of dyes in effluent which includes biological degradation, photo catalysis and adsorption tactics, etc (Das and Sarkar, 2015, Strong and West, 2011, Xiao et al., 2019a). For economical concerns, research has been moving towards more environment friendly processes. Many methods are already employed by different scientists (Kandula and Jeevanandam, 2015, M. Popescu et al., 2010, Wang et al., 2018, Cheng et al., 2019, Zhang et al., 2019)but these processes are not sufficient for the removal of pollutants as the load is very high. So there is a need to search for more advanced techniques to handle these types of pollutants. Nano technology is an advance field having advantage of biosynthesis and/or biodegradation by using bacteria's culture as well as extracts of plants due to their ability to completely degrade various types of pollutants including dyes (Senapati et al., 2005, Thyagarajan et al., 2017, Tomaszewska et al., 2013, Duncan, 2011, Liu et al., 2019a). Various types of metal nano particles can be successfully developed on nanometer scale with the most effective physic-chemical properties for a wide range of applications (Aslan et al., 2005, Roy et al., 2019, C. Chompuchan et al., 2010, Thyagarajan et al., 2017, Liang et al., 2019).

Among all metallic nanoparticles, the (AgNps) have many applications in biological as well as environmental applications. (Ag Nps) have an excellent property of degradation of different dyes (Hamedi et al., 2017). The AgNps can be produced by different techniques like physical and chemical methods (Begum et al., 2009, Mukunthan et al., 2011, Xiao et al., 2018). Unluckily these methods are very expensive or may involve dangerous chemicals for synthesis. Therefore there is also a need to develop ecofriendly methods/techniques without using hazardous chemicals. Green synthesis of AgNps is a fast increasing and economical research in nano particle synthesis. Many plant extracts can be used as a capping as well as reducing agents for the synthesis of nanoparticles, excluding the use of hazardous chemical agents and other purification techniques (Joseph and Mathew, 2014). *Azadirachta indica (*Ahmed et al., 2016b*)*, *Catharanthus roseus(*Mukunthan et al., 2011*)*, *Phoma glomerata (*Birla et al., 2009*)*, *Cissus quadrangularis (*Dhand et al., 2016*)Elettaria cardamom (*GnanaDhas GnanaJobitha et al., 2012*)*, Lantana camara flower (Fatimah and Indriani, 2018), Andean blackberry leaf (Kumar et al., 2017) Nephelium lappaceum Peel (Kumar et al., 2015) and Clove extract (Singh et al., 2010).

In the current study, the AgNps are synthesized via the green synthesis method by using extracts of tomato (T), onion (O), acacia catechu (C) and combined extracts of COT as reducing and stabilizing agents. Synthesized nanoparticles were characterized by different techniques such as UV–Vis, XRD, FTIR, DLS, SEM, EDAX, and TEM. Furthermore, the catalytic application of all synthesized products was studied for degradation of three different kinds of dyes; MR, MO and CR along with NaBH$_4$.

2. Materials and methods

2.1. Plants and chemicals

Fresh onion and tomato were purchased from a market of Harbin China. Silver nitrate (AgNO$_3$)-99.9% pure, ethanol-99%, sodium boro-hydride (NaBH$_4$) were purchased from

Aladdin chemicals China. Methyl Orange (MO), Methyl red (MR) and Congo Red (CR) and powder of Acacia catechu were purchased from the local market. Harbin China and were used without any purification. Glass wares and distilled water were used throughout the study where necessary.

2.2. Preparation of plant extracts

First of all onion and tomato were cut into small pieces and washed with distilled water thrice and then onion, tomato and acacia catechu were weighted and mixed into distilled water.20 g of onion, 20 g of tomato, and 1 g of acacia catechu powder were mixed into 200 ml distilled water in different beakers, then the mixtures were heated to boiling for 20 min to obtain the aqueous extracts. After cooling the mixtures were

filtered by whatman paper 1 and stored at 40 °C for further use.

2.3. Preparation of silver Nano-particles

Biosynthesis of AgNps was carried out according to the literature (Shankar et al., 2004, Chand et al., 2019). 1 mM solution of $AgNo_3$ was prepared by dissolving 16.987 g of $AgNO_3$ in 1L of distilled water in the beaker with the aid of sonication and was kept until used. Extracts of onion (10 ml), tomato (10 ml), acacia catechu (10 ml), and mixed extracts of COT (3 ml of each extract) were mixed with 10 ml solution of $AgNO_3$ in the beaker by using stirrer for 10 mins and kept for 24hr at room temperature. After the passage of time, the reduction of Ag ion was observed by changing of color from white to
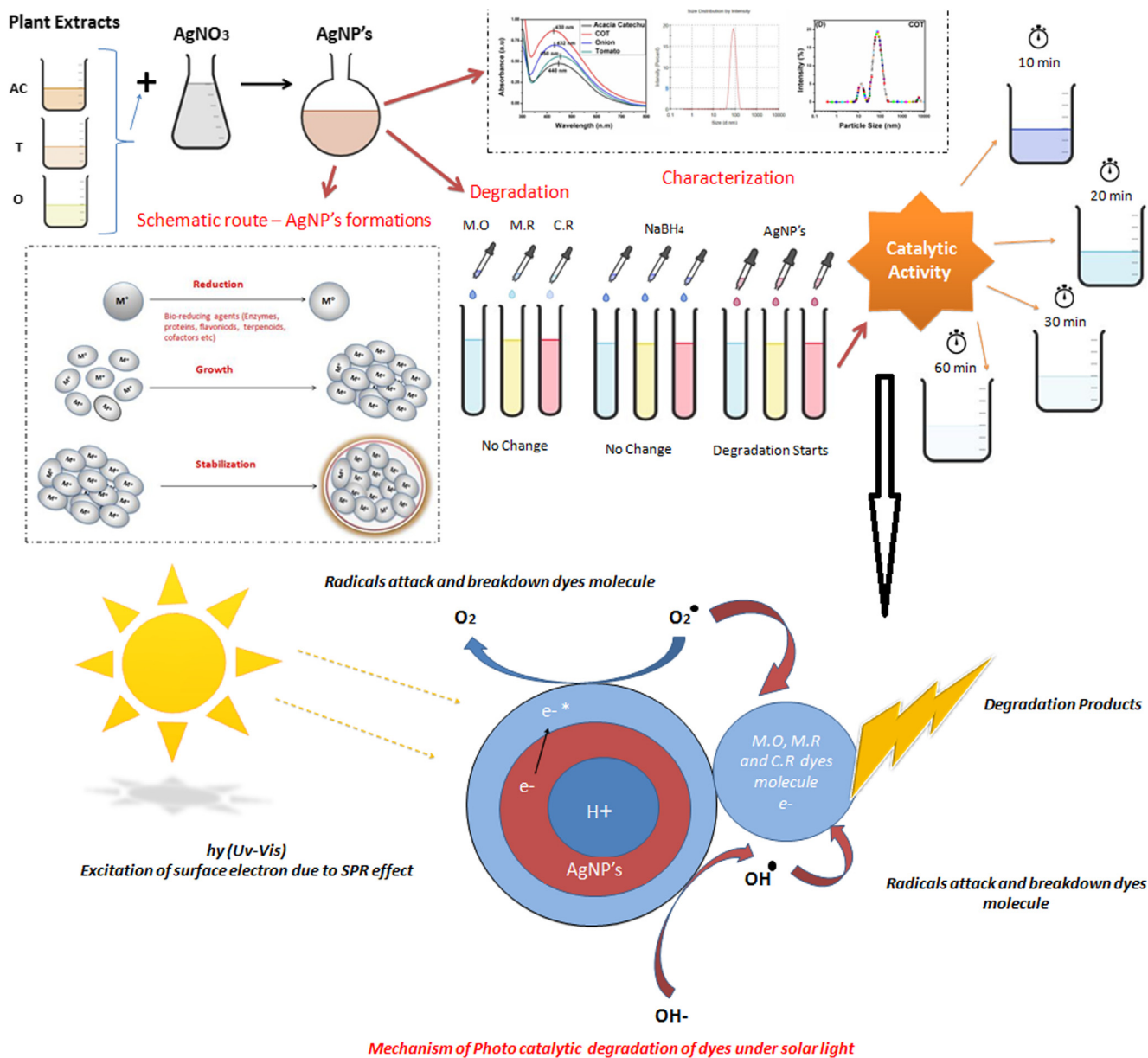

Fig. 1   Schematic representation of the mechanism of nanoparticles and degradation.
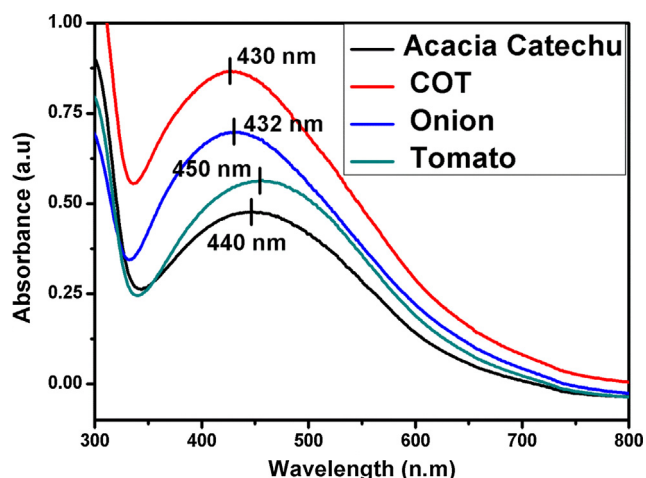
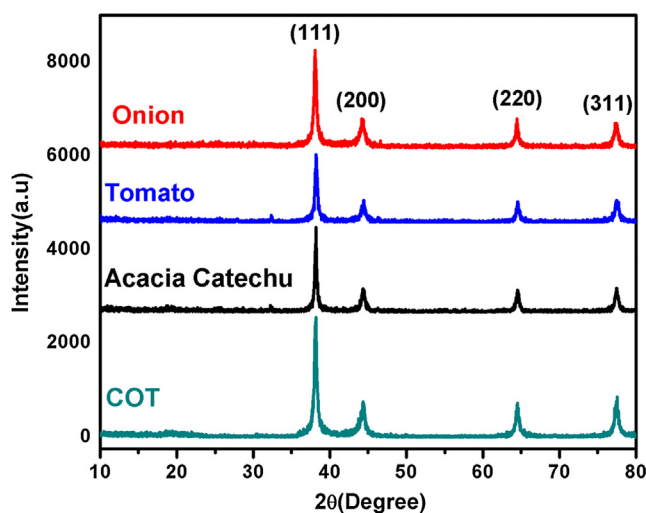**Fig. 2** UV–visible spectroscopy of silver AgNps.

Fig. 3 XRD pattern of synthesized AgNps with Onion (a), Tomato (b), Acacia catechu (c) and, COT (d).

light brown then to dark brown. The color of the solution was changing because of the formation of AgNps. After 24 hr the synthesized nano particles were centrifuged at 12000 rpm for 10mins and washed several times with ethanol and distilled water. The obtained samples were transferred to a petri dish and dried at 70 °C in a vacuum oven for 12 hr.

2.4. Characterization of synthesized silver Nano-particles

UV–vis absorption of synthesized nano particles, as well as the rate of dyes degradation, was carried out by using a TU-1901 dual-beam UV–vis spectrophotometer in the range of 190 nm to 800 nm.

The X-ray diffraction (XRD) pattern was examined for the characterization and investigation of structure and other impurities of AgNps by using Rigaku TTR at 40KV and 150 mA within 2θ area between 10 and 90°with intensity Cu-Ka radiation ($\lambda = 0.15406$ nm). In addition, particle sizes were analyzed by using the Sherrer Eq. (1).

$$\tau = \frac{k\lambda}{\beta cos\theta} \qquad (1)$$

where τ = Average size of nano particles,
   K = dimensionless shape factor, (value 0.9),
   λ = the wavelength of radiation.
   β = Full Width Half Maximum in radians and θ = angle diffraction.

The chemical constituents responsible for the reduction of AgNps and capping agents of silver nanoparticles were studied by using (FT-IR) spectroscopy. FTIR analysis was measured by using a Perkin Elmer spectrum 100 FTIR spectrometer (Waltham, MA, USA) in the range of 4000–500 cm^{-1} by crushing a small amount of AgNps with KBr powder.

Malvern ZETA Sizer nano series, UK was used to analyze the particle size and distribution of nanoparticles by dispersing them at a temperature 25 °C in water media.

The surface morphology of AgNps was analyzed using (SEM) instrument (JOEL, JSM-6480A) operated at a 20KV. The SEM test samples have been carefully collected and screened in glass bottles. The SEM copper plate was covered by conductive resin tape and particles were distributed on the tape and gold coated. Transmission electron microscopy (TEM) was used to determine the size and morphology of AgNps by using an FEI TECHNI G2 USA instrument. The test was carried out by dispersing the samples in ethanol solution through sonication for 15mins and centrifuged for 10 mins at 10000 rpm. After that the drops of AgNps were poured on the carbon-coated copper grids then left for drying naturally. A particle size distribution histogram was obtained by using a Nano Measurer Software.

2.5. Catalytic experiments

The degradation study using AgNps was investigated by making 0.1 M stock solutions of various dyes; MO, MR, and CR which were prepared in deionized water. The degradation process was performed in an open batch system at room temperature. In a typical experiment, a 10 ml dye solution was mixed with 5 ml AgNps in 250 ml conical flask with stirring for 10 mins then, 3 ml of sodium boro hydride solution were added to the above mixture. There after a small amount of each mixed solution was used to evaluate the catalytic degradation of dyes. The degradation of all dyes was completed within

Table 1 Particle size analysis of synthesized AgNps by using XRD, DLS, and TEM.

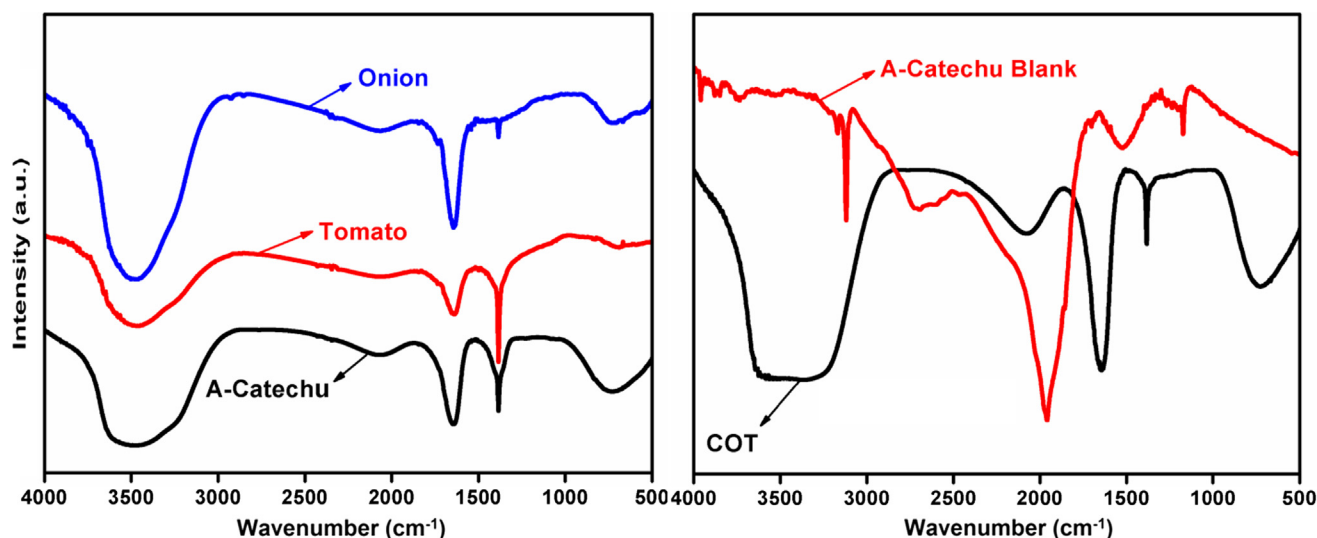| Sample Name	XRD			DLS		TEM
	FWHM (Deg)	2θ (Deg)	Particle size (nm)	Size Range (nm)	PDI	
Onion	0.26162	38.2	32.1	5–80	0.689	14.9
Tomato	0.37081	38.06	22.6	2–50	0.783	15.2
Acacia catechu	0.33015	38.22	25.4	5–80	0.465	14.88
COT	0.57611	38.16	14.5	7–80	0.378	11.7

Fig. 4 FTIR spectra of AgNps synthesized with Onion, tomato, Acacia catechu, COT, and Acacia catechu blank.
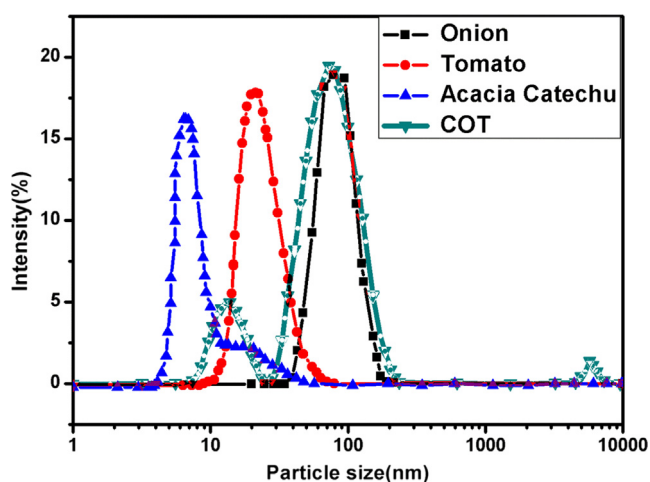

Fig. 5 DLS result of AgNps synthesized with different extracts (a) onion (b) tomato (c) Acacia catechu (d) COT.

around 5–30 min. The progress of the reaction was monitored using UV–vis spectroscopy by measuring the absorbance maxima of dyes at different time intervals. Control sets of the pure dyes without AgNps were maintained and also measured for absorbance for comparison purposes. This whole process of synthetization, as well as the mechanism of photocatalytic of AgNps, is mentioned in Fig. 1.

The degradation % of all dyes were calculated by using Eq. (2) and catalytic efficiencies were quantified by calculating the respective first-order rate constant (k) according to Eq. (3).

$$\text{Degradation}\% = \frac{A_o - A_t}{A_o} \times 100 \qquad (2)$$

$$\ln(A_o/A_t) = kt \qquad (3)$$

where A_o is the initial absorbance of dyes, A_t is the absorbance of different dyes at time t (Vizuete et al., 2016).

3. Result and discussion

3.1. UV–Visible spectroscopy

UV–Vis analysis of the synthesized AgNps with extracts of onion, tomato, acacia catechu, and mixed extracts COT are shown in Fig. 2.

In Fig. 2, the formation of AgNps synthesized by onion and tomato extracts showed the well-defined absorbance band at 432 and 450 nm. Whereas, the absorption spectra of AgNps synthesized by Acacia catechu and COT showed the absorbance bands at 440 nm and 430 nm. The good developments of bands indicate that the nano particles were successfully formed by all extracts. This clearly indicates that reducing agents are present in onion, tomato, acacia catechu, and COT extracts.

According to previous literature, the absorption peaks of silver nanoparticles are in the range of 400–450 nm (GnanaD-has GnanaJobitha et al., 2012, Bogireddy et al., 2016, de Aragão et al., 2019). These results confirmed that the synthesized AgNps of different particle sizes are formed in different extracts (Gopinath et al., 2017).

3.2. X-ray diffraction (XRD)

XRD pattern of biosynthesized AgNps by using extracts of onion, tomato, Acacia catechu and COT mixed showed the structures of all synthesized products are face centered cubic (FCC) as shown in Fig. 3. The prominent peak of AgNps was formed in the range of 2θ (36.5° to 80°), the pattern showed the four different peaks at 38.16, 44.3, 64.43 and 77.4 with corresponding lattice plane value recorded at (1 1 1), (2 0 0), (2 2 0) and (3 1 1) of FCC silver crystal. The XRD pattern of AgNps reported in the literature (Fu et al., 2016, Liu et al., 2019b, Xiao et al., 2019b) is inconsistent with the pattern shown in Fig. 3. Thus; using XRD the development of AgNps was confirmed.

The size of the nanoparticles was calculated with the help of the Scherrer Eq. (1). The average size of nano particles synthesized with onion and tomato extracts were 32.1 nm and
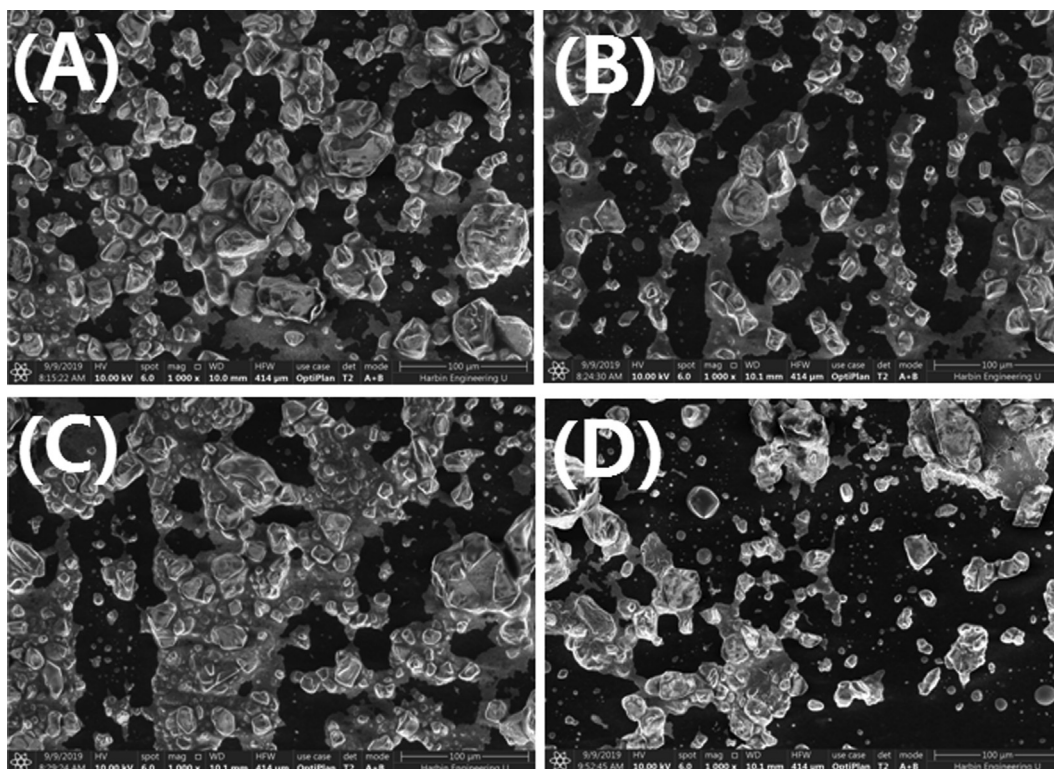
Fig. 6 Scanning electron microscopy image of AgNps using (a) onion extract and (b) Tomato extract (c) Acacia catechu and (d) COT.
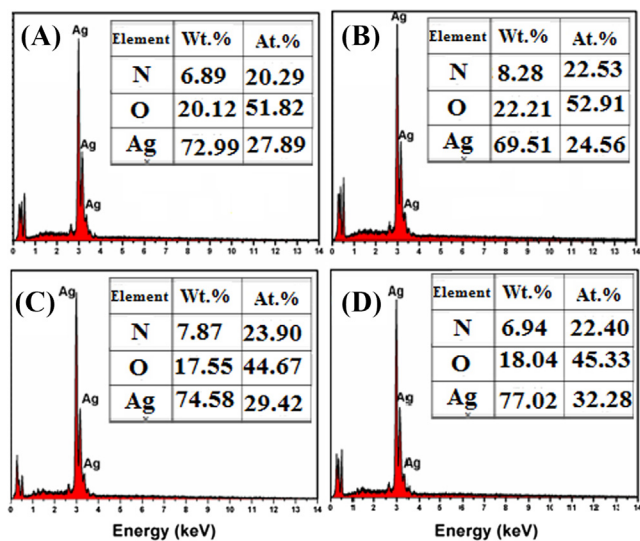

Fig. 7 EDAX image of AgNps using (a) onion extract and (b) Tomato extract (c) Acacia catechu and (d) COT.

22.6 nm, whereas in the case of AgNps synthesized with Acacia catechu and mixed COT extracts had an average particle of 25.4 and 14.5 nm, which is shown in Table 1. From the above results, it can be concluded that the smaller nanoparticles are formed in the case of COT extracts and are correlated to TEM and DLS

3.3. Fourier-transform infrared spectroscopy (FTIR)

FTIR analysis was carried out for the identification of the possible functional groups in bio molecules, present in the plant extract responsible for the reduction of the silver ion into AgNps. FTIR spectra of synthesized AgNps with plant extracts are present in Fig. 4.

FTIR spectrum of AgNps synthesized with onion, tomato and acacia catechu extracts shows different peaks at 3490, 3495, 3480, 1625, 1630, 1370, 1375, and 740 cm^{-1}. The intense and wide peak at 3500–3200 cm^{-1} denotes the N—H, O—H and H-bonded phenols and alcohols stretching vibrations of amide groups respectively. The bands appearing in the range of 1700–1600 and 1300–1000 cm^{-1} denote the C=O and C—O stretching vibrations respectively. The peak at 740 cm^{-1} is attributed to aromatic groups. While in case of AgNps synthesized with COT combined extracts and Acacia catechu extracts (without AgNO$_3$) peaks formed at 3905, 3810, 3700, 3230, 3200, 3125, 2730, 1950, 2110, 1630, 1375, 1200, and 730 cm^{-1}. As per the above discussion, the peaks formed in COT belong to N—H, O—H, AOH hydroxyl, aliphatic CAH stretching bond, NAH, N, O symmetry stretching nitro compounds and C-N stretching amines are present in these plant extracts which are responsible for the formation of AgNps. These bio molecules might be acting as reducing and stabilizing agents. According to the previous studies, the band appeared in the ranges of 1700–1600 cm^{-1} in the spectrum indicates the formation of AgNps and capped with different bio moieties (Sathishkumar et al., 2016, Harshiny et al., 2015, Sharma et al., 2017, Kalpana et al., 2019).
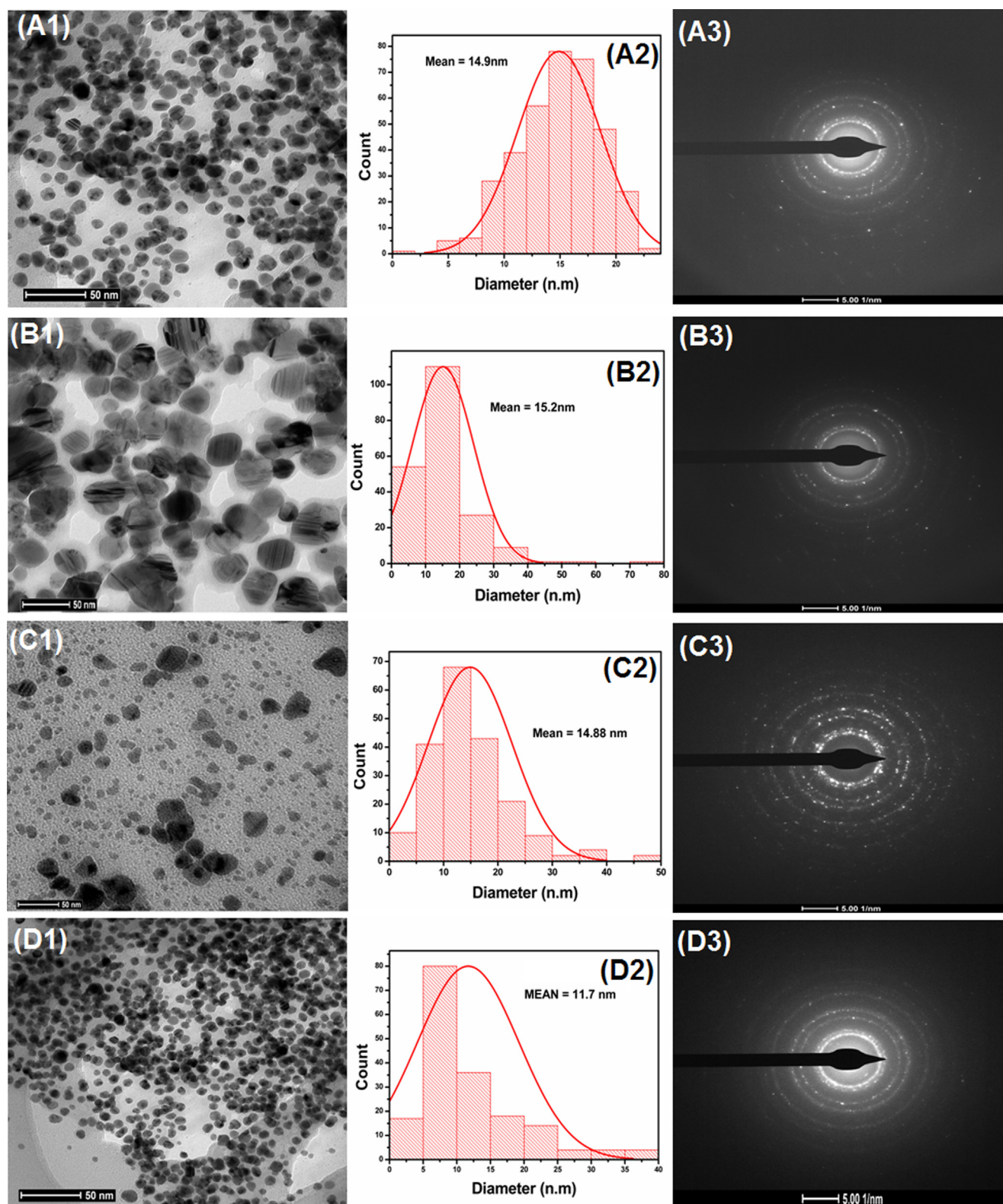
Fig. 8 TEM of AgNps synthesized with the extracts of (a) onion (b) tomato (c) Acacia catechu and (d) COT, adjacent images show the size distribution histogram and SAED pattern.

Plant extracts play a dual role; reducing and stabilizing agents in the synthesis of nanoparticles. Further, from the FTIR results, it is confirmed that the reduction of silver ion occurred due to different functional groups: terpenoids, flavones, phenolics, and polysaccharides compounds present into the plant extracts (Ahmed et al., 2016a). Terpenoids and
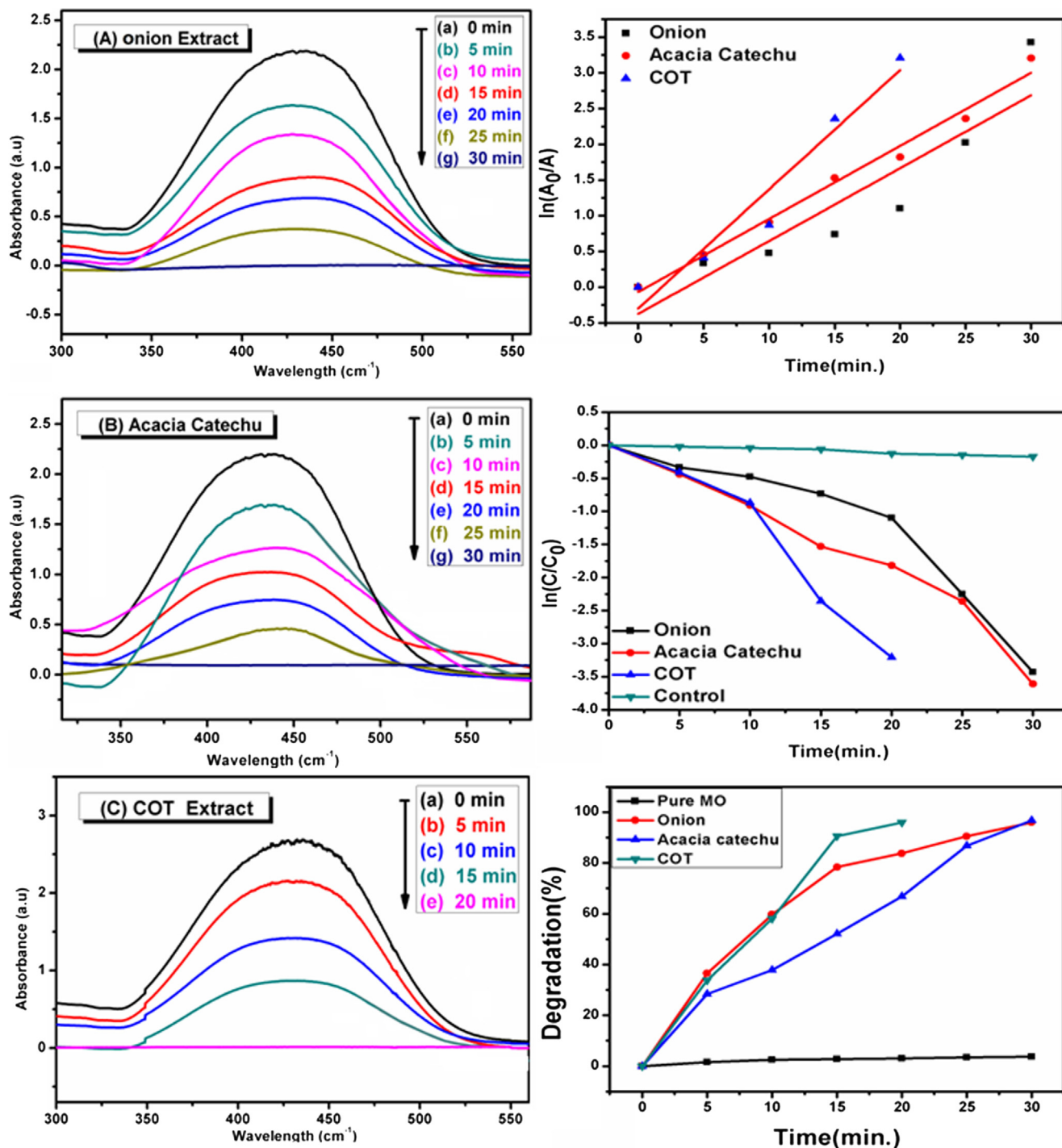
Fig. 9 UV–Vis spectra decomposition of MR by using AgNps catalyst using onion extract (a), acacia catechu (b) and COT mixed extract (c), on the other side time vs. $\ln(A_o/A)$ (d), C/C_o (e) and degradation percentage (f) of catalytic degradation of MR.

flavonoids compounds are responsible for the stabilization of AgNps and also potential constituents of onion and tomato extracts are responsible for the reduction of silver ion (Akter et al., 2018).

3.4. Dynamic light scattering (DLS)

DLS is one of the most versatile techniques used for the identification of the size of nanoparticles. The AgNps were also

Table 2 Degradation efficiencies, rate constant (k) and R^2 values of the linear fit kinetic plots for the degradation of MO, M.R, and C.R.

Dye	Sample	Time(min.)	Degradation efficiency (%DE)	Rate constant (k, min^{-1})	R^2
M.R	Onion	5–30	91	1.51×10^{-2}	0.9
	Acacia catechu	5–30	95	1.639×10^{-2}	0.924
	COT	5–20	97	3.547×10^{-2}	0.911
M.O	Onion	5–30	89	1.752×10^{2}	0.938
	Acacia catechu	5–30	91	1.911×10^{-2}	0.98
	COT	5–20	95	2.326×10^{-2}	0.926
C.R	Onion	2–28	96	1.219×10^{-2}	0.964
	Acacia catechu	2–20	97	2.698×10^{-2}	0.931
	COT	2–15	98.5	3.078×10^{-2}	0.942

characterized by using DLS. The average particle size distribution of AgNps is shown in Fig. 5.The average particle size distribution in all cases was in the range of 2–80 nm which is mentioned in Table 1. This study is acceptable because the DLS measures only the diameter and not the actual size of the nanoparticles. The single peak indicates the uniform distribution of nanoparticles (Sharma et al., 2017).

3.5. Scanning electron microscopy (SEM))-energy dispersive X-ray spectrometer (EDX)

Surface morphology and topography of the AgNps were observed by using SEM. Fig. 6 depicts that the morphology of the synthesized AgNps is near to be spherical in shape and in agglomerated condition.

SEM images were examined at a magnification of 50,000 and scale of 100 nm show that the sizes of the primary synthesized particles are in the nano size range. (Kumar et al., 2014). According to the EDX result, the green synthesized AgNps also produce a strong signal at 3 keV as shown in Fig. 7, which confirms the existence of silver (Ag) and the organic components which are present along with the Nps (Bello et al., 2017). The presence of other components is due to the plant extracts (COT).

3.6. Transmission electron microscopy (TEM)

The AgNps was also characterized by TEM.TEM is also one of the most advanced image measurement techniques to distinguish the morphology, size, and shape of nanoparticles synthesized by different methods (Ravichandran et al., 2019). TEM images of the synthesized products were measured in the range of 50 nm. The images of TEM with the particle size distributions displayed by the histogram curves in Fig. 8(a1–d1) and Fig. 8(a2–d2) and SAED pattern portrayed in 9 (a3-d3).

In Fig. 8, the nanoparticles synthesized with onion (a2) and tomato (b2) extracts show 14.9 and 15.2 nm average particle sizes. While AgNps synthesized with Acacia catechu and COT extracts have average particle sizes of 14.88 and 11.7 nm as shown in Fig. 8 (c2 and d2) and Table 1.

According to the previous study, the AgNps particle size can be changed according to concentration, environmental effect, and varying pH from acid to basic level (Verma and Mehata, 2016). The above results of TEM and SEM correlated with previous described UV–Vis and DLS results. From the

above results in Fig. 8, it can be concluded that spherical shaped AgNps in all cases were formed with nano-size up to 50 nm with irregular morphologies and poly dispersed character.

3.7. Catalytic application

3.7.1. Degradation of methyl red

The efficiency of AgNps as nano catalysts for the degradation of MR using nanoparticles along with $NaBH_4$ as a reducing agent was studied. MR is used in dying industries as colorants and selected as a model substrate for catalytic application. These dying industries release dye effluents in the water sources and water pollutes. MR is also a dangerous pollutant, which creates pollution to the environment and, therefore, proper treatment of MR is required.

The catalytic action on MR was carried out in the presence of AgNps synthesized with onion, tomato, Acacia catechu, and COT mixed extracts. We observed that AgNps synthesized with onion, tomato and acacia catechu have almost the same effect on dye degradation that's why we only choose to compare onion and acacia catechu to COT and excluded tomato as shown in Fig. 9. The absorption peak of pure MR in the distilled water was noted 445 nm (Jyoti and Singh, 2016). Subsequently, the maxima absorption was observed in the presence of AgNps during an incubation time period of 30 min using UV–visible spectroscopy as shown in Fig. 9. Results show that the maxima absorption was decreased in all cases within 30 mins except for COT. In COT, degradation occurs within a shorter period of time (20 min). This can be clearly shown that the complete dye degradation takes place by adding the AgNps synthesized with onion, Acacia catechu, COT mixed extracts along with $NaBH_4$. Degradation percentage was calculated by using Eq. (2) and a simple kinetic study of the dye degradation of MR was carried out by using pseudo first order reaction as per Eq. (3). In this study, the rate constant and R^2 value of each product was calculated from Fig. 9 (d) and shown in Table 2. Fig. 9(e) shows the high conversion rate attained by COT extract compared to other individual extracts. It depicts the decrease in dye concentration over time. Degradation percentage of MR dye is shown in Fig. 9 (f) and the values are recorded in Table 2. From these results, it can be observed that AgNps synthesized with COT is more effective as compared to AgNps synthesized with onion, tomato and acacia catechu. This is because of different components present
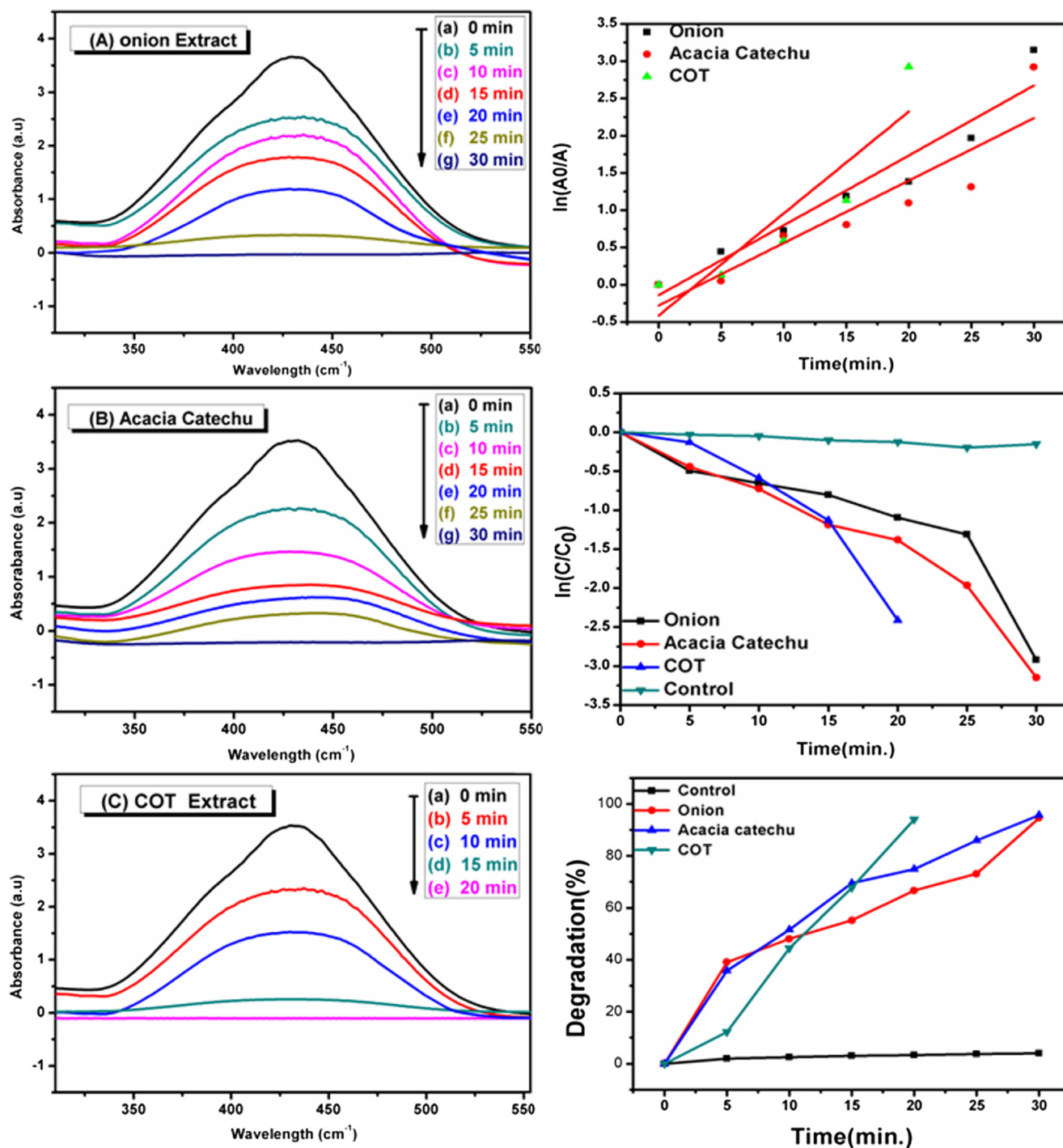
Fig. 10 UV–Vis spectra decomposition of MO by using AgNps catalyst synthesized from onion extract (a), acacia catechu (b) and COT mixed extract (c).On the other side, time vs. ln(A_o/A) plot(d), C/C_o (e) and degradation percentage (f) of catalytic degradation of MO using: onion, Acacia catechu and COT mixed extract.

in the COT mixed extracts as per FTIR in addition to having smaller particle sizes as per the TEM test compared to the other products.

3.7.2. Degradation of methyl orange

The catalytic action of the AgNps synthesized with onion, tomato, acacia catechu and COT extracts for the degradation of the MO dye along with $NaBH_4$ were evaluated MO was

selected as a model for azo dye, widely used as an organic dye in textile, printing, and paper dying.

In Fig. 10(a–c), it can easily be noted that the peak of the pure MO dye in absence of nanoparticles and $NaBH_4$ appears at 460 nm (Bogireddy et al., 2016, Sakir and Onses, 2019). After adding AgNps and $NaBH_4$, it was observed that the peak of MO gradually decreases with time and a complete degradation occurs within 30 min in case of the AgNps
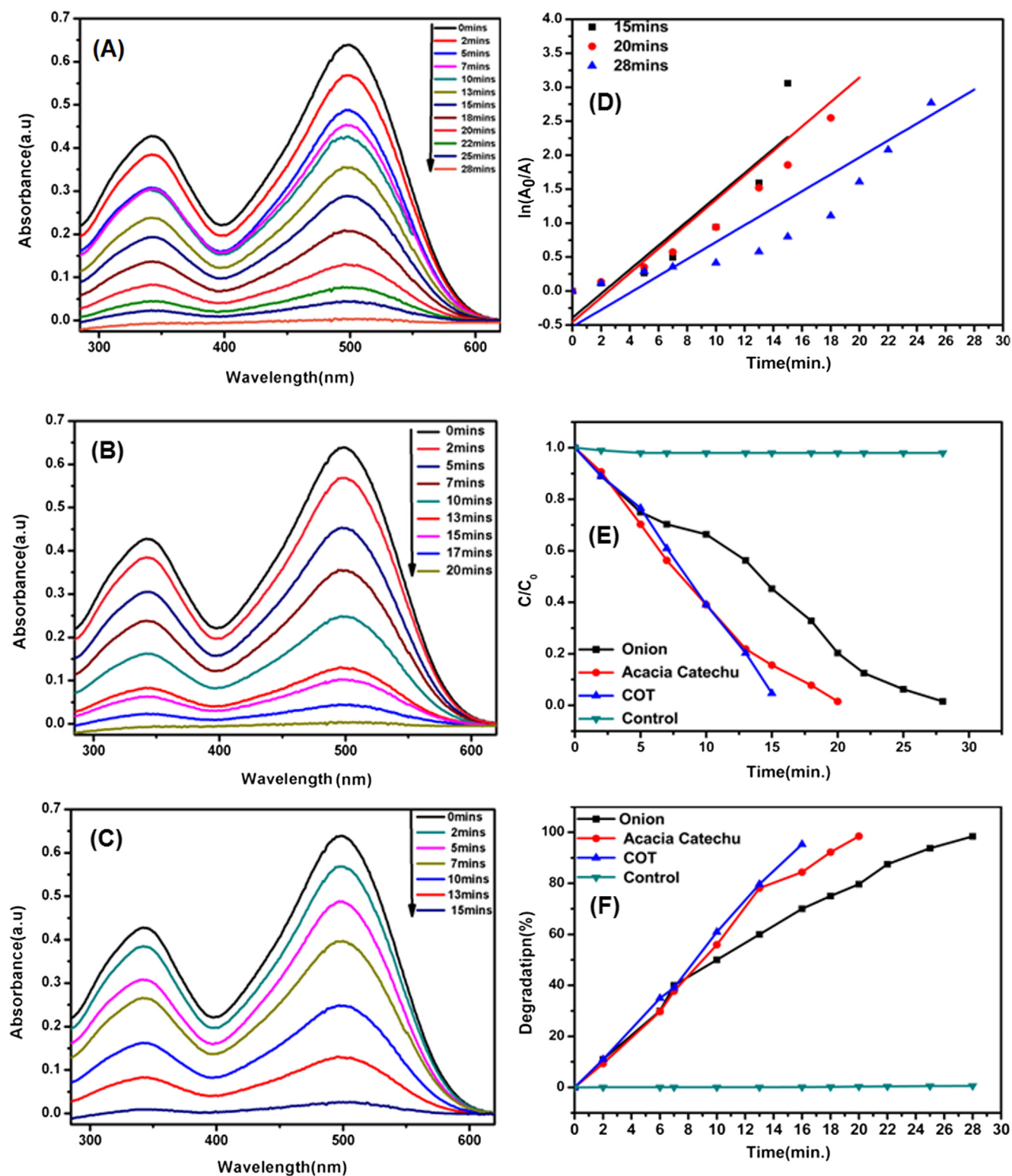
Fig. 11 UV–Vis spectra decomposition of CR by using AgNps catalyst obtained from onion extract (a), acacia catechu (b) and COT mixed extract (c). The plots on the right side show the corresponding time vs. ln(A$_o$/A) (d), C/C$_o$ (e) and degradation percentage (f) for the catalytic degradation of CR.

synthesized with onion, tomato and acacia catechu. Whereas, a complete degradation was observed within 20 min in case of AgNps synthesized with COT mixed extracts. The degradation percentages and kinetics of the degradation reaction was calculated by using Eq. (2) and Eq. (3), respectively. The rate constant and R^2 value of each product were calculated and

shown in Fig. 10(d) and Table 2. These values were obtained from the pseudo first-order linear fit graphs. Degradation efficiencies of different products are shown in Fig. 10(f) and Table 2. The high conversion rate attained by COT extract compared to other individual extracts. It depicts the decrease in the dye concentration over time as shown in Fig. 10(e). According to results, it can be concluded that AgNps synthesized with mixed COT extract have more efficiency as compared to other AgNps. The linear fit graph of time vs $\ln(A_O/A)$ reveals complete degradation of the MO dye using AgNps synthesized with onion, Acacia catechu, and COT mixed extracts as depicted in Fig. 10(d).

3.7.3. Degradation of congo red

CR is a highly toxic and carcinogenic anionic dye. It belongs to a group of azo dyes derived from benzylamine. The presence of CR dye in the waste water would be very harmful to the aquatic environment.

The catalytic degradation of CR dye using AgNps as a catalyst was investigated by UV–Vis spectra during the given time frame. Fig. 11(a–c) represents the degradation of CR through the reduction in the main peak of the pure CR dye which appears at 497 nm (Umamaheswari et al., 2018). The degradation efficiency was calculated by using Eq. (2) and shown in Fig. 11(f). The degradation kinetics were found to follow a pseudo first-order reaction as per Eq. (3). In this study, the rate constant and R^2 value of each product was calculated and shown in Fig. 11(d) and Table 2 as well as the higher conversion rate attained by COT extract compared to other individual extracts. It depicts the decrease in the dye concentration over time as shown in Fig. 11(e).

AgNps synthesized with onion, acacia catechu and COT mixed extracts are successfully used as photo catalysts because of the high surface to volume ratio, eco-friendly, low cast and unique method of treatment for many toxic dye waste. According to results, it is shown that the complete degradation occurs within 28 min in case of AgNps synthesized with onion and acacia catechu, whereas, complete degradation was observed within 15 min with COT mixed extracts. According to literature, the catalytic activity of nanoparticles depends on the shape, size and crystal structure of particles, as well as different plant composition (Wahi et al., 2005).

4. Conclusions

In this study, AgNps were prepared by using a green route in extracts of onion, tomato acacia catechu and COT mixed extracts. This eco-friendly procedure was relatively inexpensive, rapid and easy and did not require any toxic chemicals. The biosynthesis process was very advantageous over other chemical methods of synthesis AgNps. The prepared nano particles were crystalline and spherical in shape with size ± 50 nm. Furthermore, these nano particles were used as nano catalysts in the process of degradation of four different dyes like MO, MR, and CR room temperature. In the presence of AgNps synthesized with onion and acacia catechu, MO and MR dyes were completely degraded within very short reactive time (20 min) where as in case of CR dye was completely degraded reactive time (15 min) Furthermore, AgNps synthesized with COT mixed have increased effect on degradation of all dyes as compared to other products synthesized alone in any one

extract. Therefore, this study provides an eco-friendly method for controlled synthesis of shape and size-dependent AgNps, which can be used in effluent treatment (dye degradation) of different types of industries like textile, paper, plastic, paints and many other chemical industries.

Declaration of Competing Interest

The authors declare no conflict of interest.

References

Ahmed, S., Ahmad, M., Swami, B.L., Ikram, S., 2016a. A review on plants extract mediated synthesis of silver nanoparticles for antimicrobial applications: a green expertise. J. Adv. Res 7, 17–28. https://doi.org/10.1016/j.jare.2015.02.007.

Ahmed, S., Saifullah, Ahmad, M., Swami, B.L., Ikram, S., 2016b. Green synthesis of silver nanoparticles using Azadirachta indica aqueous leaf extract. J. Radiat. Res. Appl. Sci. 9, 1–7. https://doi.org/10.1016/j.jrras.2015.06.006.

Akter, M., Sikder, M.T., Rahman, M.M., Ullah, A., Hossain, K.F.B., Banik, S., Hosokawa, T., Saito, T., Kurasaki, M., 2018. A systematic review on silver nanoparticles-induced cytotoxicity: physicochemical properties and perspectives. J. Adv. Res 9, 1–16. https://doi.org/10.1016/j.jare.2017.10.008.

Aslan, K., Lakowicz, J.R., Geddes, C.D., 2005. Metal-enhanced fluorescence using anisotropic silver nanostructures: critical progress to date. Anal. Bioanal. Chem 382, 926–933. https://doi.org/10.1007/s00216-005-3195-3.

Begum, N.A., Mondal, S., Basu, S., Laskar, R.A., Mandal, D., 2009. Biogenic synthesis of Au and Ag nanoparticles using aqueous solutions of Black Tea leaf extracts. Colloids. Surf. B. Biointerfaces 71, 113–118. https://doi.org/10.1016/j.colsurfb.2009.01.012.

Bello, B.A., Khan, S.A., Khan, J.A., Syed, F.Q., Mirza, M.B., Shah, L., Khan, S.B., 2017. Anticancer, antibacterial and pollutant degradation potential of Silver nanoparticles from hyphaene thebaica. Biochem. Biophys. Res. Commun. doi: 10.1016/.

Birla, S.S., Tiwari, V.V., Gade, A.K., Ingle, A.P., Yadav, A.P., Rai, M.K., 2009. Fabrication of silver nanoparticles by Phoma glomerata and its combined effect against Escherichia coli, Pseudomonas aeruginosa and Staphylococcus aureus. Lett. Appl. Microbiol 48, 173–179. https://doi.org/10.1111/j.1472-765X.2008.02510.x.

Bogireddy, N.K.R., Kiran Kumar, H.A., Mandal, B.K., 2016. Biofabricated silver nanoparticles as green catalyst in the degradation of different textile dyes. J. Environ. Chem. Eng. 4, 56–64. https://doi.org/10.1016/j.jece.2015.11.004.

Chand, K., Abro, M.I., Aftab, U., Shah, A.H., Lakhan, M.N., Cao, D., Mehdi, G., ALI Mohamed, A.M., 2019. Green synthesis characterization and antimicrobial activity against Staphylococcus aureus of silver nanoparticles using extracts of neem, onion and tomato. RSC Adv. 9, 17002–17015. https://doi.org/10.1039/c9ra01407a.

Cheng, Y., Li, H., Fang, C., Wang, K., Chen, J., Su, J., Zheng, F., 2019. Green synthesis of fluorescent Ag-anionic polyacrylamide nanoparticles gels solution with high stability via a simple template method. Results Phys. https://doi.org/10.1016/j.rinp.2019.102636.

Chompuchan, C., Satapanajaru, T., Suntornchot, P., Pengthamkeerati, P., 2010. Decolorization of Reactive Black 5 and Reactive Red 198 using nanoscale zerovalent iron. Int. J. Civil Environ. Eng 2, 123–127.

Das, R., Sarkar, S., 2015. Optical properties of silver nano-cubes. Opt. Mater. 48, 203–208. https://doi.org/10.1016/j.optmat.2015.07.038.

De Aragão, A.P., De Oliveira, T.M., Quelemes, P.V., Perfeito, M.L. G., Araújo, M.C., Santiago, J.D.A.S., Cardoso, V.S., Quaresma, P., De Souza De Almeida Leite, J.R., Da Silva, D.A., 2019. Green synthesis of silver nanoparticles using the seaweed Gracilaria birdiae and their antibacterial activity. Arab. J. Chem. 12, 4182–4188. https://doi.org/10.1016/j.arabjc.2016.04.014.

Dhand, V., Soumya, L., Bharadwaj, S., Chakra, S., Bhatt, D., Sreedhar, B., 2016. Green synthesis of silver nanoparticles using Coffea arabica seed extract and its antibacterial activity. Mater. Sci. Eng. C. Mater. Biol. Appl. 58, 36–43. https://doi.org/10.1016/j.msec.2015.08.018.

Duncan, T.V., 2011. Applications of nanotechnology in food packaging and food safety: barrier materials, antimicrobials and sensors. J. Colloid. Interface. Sci 363, 1–24. https://doi.org/10.1016/j.jcis.2011.07.017.

Fatimah, I., Indriani, N., 2018. Silver nanoparticles synthesized using lantana camara flower extract by reflux, microwave and ultrasound methods. Chem. J. Moldova 13, 95–102. https://doi.org/10.19261/cjm.2017.461.

Fouad, D.E., Zhang, C., Mekuria, T.D., Bi, C, Zaidi, A.A., Shah, A. H. 2019b. Effects of sono-assisted modified precipitation on the crystallinity, size, morphology, and catalytic applications of hematite (alpha-Fe2O3) nanoparticles: a comparative study. Ultrason. Sonochem., 59, 104713, doi: http://doi.org/10.1016/j.rinp.2019.01.005.

Fouad, D.E., Zhang, C., El-Didamony, H., Yingnan, L., Mekuria, T. D., Shah, A.H., 2019a. Improved size, morphology and crystallinity of hematite (α-Fe2O3) nanoparticles synthesized via the precipitation route using ferric sulfate precursor. Results. Phys. 12, 1253–1261. https://doi.org/10.1016/j.ultsonch.2019.104713.

Fu, L.-H., Deng, F., MA, M.-G., Yang, J. 2016. Green synthesis of silver nanoparticles with enhanced antibacterial activity using holocellulose as a substrate and reducing agent. RSC Adv., 6, 28140–28148, doi: http://doi.org/10.1039/c5ra27421d.

Gnanajobitha, Gnanadhas, Annadurai, Gurusamy, Kannan, C., 2012. Green synthesis of silver nanoparticle using elettaria cardamomum and assessment of its antimicrobial activity. Int J. Pharma Sci. Res. 3, 323–330.

Gopinath, V., Priyadarshini, S., Loke, M.F., Arunkumar, J., Marsili, E., Mubarakali, D., Velusamy, P., Vadivelu, J., 2017. Biogenic synthesis, characterization of antibacterial silver nanoparticles and its cell cytotoxicity. Arabian. J. Chem. 10, 1107–1117. https://doi.org/10.1016/j.arabjc.2015.11.011.

Hamedi, S., Shojaosadati, S.A., Mohammadi, A., 2017. Evaluation of the catalytic, antibacterial and anti-biofilm activities of the Convolvulus arvensis extract functionalized silver nanoparticles. J. Photochem. Photobiol. B 167, 36–44. https://doi.org/10.1016/j.jphotobiol.2016.12.025.

Harshiny, M., Matheswaran, M., Arthanareeswaran, G., Kumaran, S., Rajasree, S., 2015. Enhancement of antibacterial properties of silver nanoparticles– ceftriaxone conjugate through Mukia maderaspatana leaf extract mediated synthesis. Ecotoxicol. Environ. Saf. 121, 135–141. https://doi.org/10.1016/j.ecoenv.2015.04.041.

Joseph, S., Mathew, B., 2014. Microwave assisted biosynthesis of silver nanoparticles using the rhizome extract of alpinia galanga and evaluation of their catalytic and antimicrobial activities. J. Nanopart. 2014, 1–9. https://doi.org/10.1155/2014/967802.

Jyoti, K., Singh, A., 2016. Green synthesis of nanostructured silver particles and their catalytic application in dye degradation. J. Genet. Eng. Biotechnol 14, 311–317. https://doi.org/10.1016/j.jgeb.2016.09.005.

Kalpana, D., Han, J.H., Park, W.S., Lee, S.M., Wahab, R., Lee, Y.S., 2019. Green biosynthesis of silver nanoparticles using Torreya nucifera and their antibacterial activity. Arabian. J. Chem. 12, 1722–1732. https://doi.org/10.1016/j.arabjc.2014.08.016.

Kandula, S., Jeevanandam, P., 2015. Sun-light-driven photocatalytic activity by ZnO/Ag heteronanostructures synthesized via a facile thermal decomposition approach. RSC. Adv. 5, 76150–76159. https://doi.org/10.1039/c5ra14179f.

Kumar, P.P.N.V., Pammi, S.V.N., Kollu, P., Satyanarayana, K.V.V., Shameem, U., 2014. Green synthesis and characterization of silver nanoparticles using Boerhaavia diffusa plant extract and their anti bacterial activity. Ind. Crops. Prod. 52, 562–566. https://doi.org/10.1016/j.indcrop.2013.10.050.

Kumar, B., Smita, K., Cumbal, L., Angulo, Y., 2015. Fabrication of silver nanoplates using Nephelium lappaceum (Rambutan) peel: A sustainable approach. J. Mol. Liq. 211, 476–480. https://doi.org/10.1016/j.molliq.2015.07.067.

Kumar, B., Smita, K., Cumbal, L., Debut, A., 2017. Green synthesis of silver nanoparticles using Andean blackberry fruit extract. Saudi. J. Biol. Sci 24, 45–50. https://doi.org/10.1016/j.sjbs.2015.09.006.

Liang, Z., Zhao, R., Qiu, T., Zou, R., Xu, Q., 2019. Metal-organic framework-derived materials for electrochemical energy applications. EnergyChem 1. https://doi.org/10.1016/j.enchem.2019.100001.

Liu, G., Sheng, Y., Ager, J.W., Kraft, M., Xu, R., 2019a. Research advances towards large-scale solar hydrogen production from water. EnergyChem 1. https://doi.org/10.1016/j.enchem.2019.100014.

Liu, H., Sun, Y., Zhang, H., Wang, J., Wei, J., 2019b. Hydrodynamic cavitation enhanced biosynthesis of silver nanoparticles at room temperature and its mechanism. Mater. Lett. 236, 387–389. https://doi.org/10.1016/j.matlet.2018.10.103.

Mukunthan, K.S., Elumalai, E.K., Patel, T.N., Murty, V.R., 2011. Catharanthus roseus: a natural source for the synthesis of silver nanoparticles. Asian Pacific. J. Trop. Biomed. 1, 270–274. https://doi.org/10.1016/s2221-1691(11)60041-5.

Nithya, R., Ragunathan, R., thya and Ragunathan 2009. Synthesis of silver nanoparticle using pleurotus sajor caju and its antimicrobial study. Digest J. Nanomater. Biostruct. 4, 623–629.

Popescu, M., Velea, A., Lőrinczi, A., 2010. Biogenic production of nanoparticles. Digest. J. Nanomater. Biostruct. 5, 1035–1040.

Ravichandran, V., Vasanthi, S., Shalini, S., Shah, S.A.A., Tripathy, M., Paliwal, N., 2019. Green synthesis, characterization, antibacterial, antioxidant and photocatalytic activity of Parkia speciosa leaves extract mediated silver nanoparticles. Results. Phys. 15. https://doi.org/10.1016/j.rinp.2019.102565.

Roy, A., Bulut, O., Some, S., Mandal, A.K., Yilmaz, M.D., 2019. Green synthesis of silver nanoparticles: biomolecule-nanoparticle organizations targeting antimicrobial activity. RSC. Adv. 9, 2673–2702. https://doi.org/10.1039/c8ra08982e.

Sakir, M., Onses, M.S., 2019. Solid substrates decorated with Ag nanostructures for the catalytic degradation of methyl orange. Results. Phys. 12, 1133–1141. https://doi.org/10.1016/j.rinp.2018.12.084.

Sathishkumar, P., Preethi, J., Vijayan, R., Yusoff, A.R.M., Ameen, F., Suresh, S., Balagurunathan, R., Palvannan, T., 2016. Anti-acne, anti-dandruff and anti-breast cancer efficacy of green synthesised silver nanoparticles using Coriandrum sativum leaf extract. J. Photochem. Photobiol. B 163, 69–76. https://doi.org/10.1016/j.jphotobiol.2016.08.005.

Senapati, S., Ahmad, A., Khan, M.I., Sastry, M., Kumar, R., 2005. Extracellular biosynthesis of bimetallic Au-Ag alloy nanoparticles. Small 1, 517–520. https://doi.org/10.1002/smll.200400053.

Shankar, S.S., Rai, A., Ahmad, A., Sastry, M., 2004. Rapid synthesis of Au, Ag, and bimetallic Au core-Ag shell nanoparticles using Neem (Azadirachta indica) leaf broth. J. Colloid. Interface. Sci 275, 496–502. https://doi.org/10.1016/j.jcis.2004.03.003.

Sharma, P., Pant, S., Rai, S., Yadav, R.B., Dave, V., 2017. Green Synthesis of Silver Nanoparticle Capped with Allium cepa and Their Catalytic Reduction of Textile Dyes: An Ecofriendly Approach. J. Polym. Environ. 26, 1795–1803. https://doi.org/10.1007/s10924-017-1081-7.

Singh, A.K., Talat, M., Singh, D.P., Srivastava, O.N., 2010. Biosynthesis of gold and silver nanoparticles by natural precursor clove and their functionalization with amine group. J. Nanopart. Res. 12, 1667–1675. https://doi.org/10.1007/s11051-009-9835-3.

Strong, L.E., West, J.L., 2011. Thermally responsive polymer-nanoparticle composites for biomedical applications. Wiley. Interdiscip. Rev. Nanomed. Nanobiotechnol 3, 307–317. https://doi.org/10.1002/wnan.138.

Thyagarajan, L.P., Sudhakar, S., Meenambal, T. 2017. Bioremediation of Congo-Red Dye by Using Silver Nanoparticles Synthesized from Bacillus sps. Bioremed. Sustain. Technol. Cleaner Environ.

Tomaszewska, E., Soliwoda, K., Kadziola, K., Tkacz-szczesna, B., Celichowski, G., Cichomski, M., Szmaja, W., Grobelny, J., 2013. Detection limits of DLS and UV-vis spectroscopy in characterization of polydisperse nanoparticles colloids. J. Nanomater. 2013, 1–10. https://doi.org/10.1155/2013/313081.

Umamaheswari, C., Lakshmanan, A., Nagarajan, N.S., 2018. Green synthesis, characterization and catalytic degradation studies of gold nanoparticles against congo red and methyl orange. J. Photochem. Photobiol. B 178, 33–39. https://doi.org/10.1016/j.jphotobiol.2017.10.017.

Verma, A., Mehata, M.S., 2016. Controllable synthesis of silver nanoparticles using Neem leaves and their antimicrobial activity. J. Radiat. Res. Appl. Sci. 9, 109–115. https://doi.org/10.1016/j.jrras.2015.11.001.

Vizuete, K.S., Kumar, B., Vaca, A.V., Debut, A., Cumbal, L., 2016. Mortiño (Vaccinium floribundum Kunth) berry assisted green synthesis and photocatalytic performance of Silver-Graphene nanocomposite. J. Photochem. Photobiol. A 329, 273–279. https://doi.org/10.1016/j.jphotochem.2016.06.030.

Wahi, R.K., Yu, W.W., Liu, Y., Mejia, M.L., Falkner, J.C., Nolte, W., Colvin, V.L., 2005. Photodegradation of Congo Red catalyzed by nanosized TiO2. J. Mol. Catal. A: Chem. 242, 48–56. https://doi.org/10.1016/j.molcata.2005.07.034.

Wang, L., Lu, F., Liu, Y., Wu, Y., Wu, Z., 2018. Photocatalytic degradation of organic dyes and antimicrobial activity of silver nanoparticles fast synthesized by flavonoids fraction of Psidium guajava L. leaves. J. Mol. Liq. 263, 187–192. https://doi.org/10.1016/j.molliq.2018.04.151.

Xiao, X., Li, Q., Yuan, X., Xu, Y., Zheng, M., Pang, H., 2018. Ultrathin Nanobelts as an Excellent Bifunctional Oxygen Catalyst: Insight into the Subtle Changes in Structure and Synergistic Effects of Bimetallic Metal-Organic Framework. Small Methods 2. https://doi.org/10.1002/smtd.201800240.

Xiao, X., Zou, L., Pang, H., Xu, Q., 2019b. Synthesis of micro-/nanoscaled metal-organic frameworks and their direct electrochemical applications. Chem. Soc. Rev. https://doi.org/10.1039/c7cs00614d.

Xiao, X., Zhang, G., Xu, Y., Zhang, H., Guo, X., Liu, Y., Pang, H., 2019a. Correction: A new strategy for the controllable growth of MOF@PBA architectures. J. Mater. Chem. A 7, 20436–20437. https://doi.org/10.1039/c9ta90211b.

Zhang, S., Zhao, Y., Shi, R., Waterhouse, G.I.N., Zhang, T., 2019. Photocatalytic ammonia synthesis: recent progress and future. EnergyChem 1. https://doi.org/10.1016/j.enchem.2019.100013.